# Nanoparticles of Anastrozole: Fabrication and Assessment for Transdermal Delivery

Kamil K. Atiyah Altameemi*[1] and Shaimaa N. Abd-Alhammid**[2]

1 Ministry of Health, Thi-Qar Health Directorate, Thi-Qar, Iraq.
2 Department of Pharmaceutics, College of Pharmacy, University of Baghdad, Baghdad, Iraq.
* Corresponding author: email: Kamel.kareem1100a@copharm.uobaghdad.edu.iq
**Received (20\01\2022), Accepted 20\03\2022)**

## Abstract

Anastrozole, a third-generation aromatase inhibitor, it treats postmenopausal breast cancer in estrogen receptor-positive patients. The restrictions of anastrozole are involved low aqueous solubility, first-pass effect and stomach troubles. In the current work, anastrozole nanoparticles were developed to manage the transdermal delivery of anastrozole as an alternative to the oral route and to increase patient compliance.

Method: anastrozole nanoparticles were made by nanoprecipitation utilizing Kollicoat MAE100-55 as the polymer and poloxamer 188, polyvinyl pyrrolidone-K30, and hydroxy propyl methyl cellulose E5 as stabilizers. Polymer and stabilizer concentrations and stabilizer types were investigated for their effects on nanoparticle physical parameters such as particle size, zeta potential, entrapment efficiency and *in-vitro* release. Morphological and compatibility examinations, as well as an ex *vivo* permeation investigation via rat abdomen skin to investigate the effect of solid polymeric microneedles on drug flux, were also conducted.

Results: The results showed nanoprecipitation can make polymeric nanoparticles. Prepared polymeric nanoparticles ranged in size from 47.41±10.1nm to 541.3±23.6 nm and had a negative zeta potential. Entrapment efficiency ranged from 37.67% to 76.3%. A spherical, uniform shape was seen in transmission electron microscopy of formula (F2). Formula (F2) was chosen for further evaluation due to its small particle size, high entrapment efficiency percent, and 4-hour release pattern. The compatibility analysis didn't consider anastrozole's interaction with other

parts. The permeation study found polymer microneedles increased drug penetration into rat skin compared to nanoparticles.

Conclusion: Combining polymeric nanoparticles and microneedles increased the transdermal absorption and penetration of anastrozole, as an alternative to the oral route, to increase patient compliance and minimized side effects.

**Keywords**: Anastrozole, Polymeric nanoparticles, Nanoprecipitation method, Poloxamer 188.

**الجسيمات النانوية من أناستروزول: تصنيع وتقييم لا عطائها عن طريق الجلد**

**كامل كريم عطيه التميمي*[1] و شيماء نزار عبد الحميد**[2]**

1وزارة الصحة، دائرة صحة ذي قار، ذي قار، العراق.

2فرع الصيدلانيات ، كلية الصيدلة ، جامعة بغداد ، بغداد ،العراق..

*المؤلف المراسل

الكلمات المفتاحية :أناستروزول، الجسيمات النانوية، طريقة الترسيب النانوية،Poloxamer 188

الخلاصة

أناستروزول ، مثبطات الجيل الثالث من الأروماتاز ، يعالج سرطان الثدي بعد سن اليأس في المرضى الذين لديهم مستقبلات هرمون الاستروجين. تشمل قيود أناستروزول قابلية منخفضة للذوبان في الماء وتأثير المرور في الكبد ومشاكل في المعدة. في العمل الحالي ، تم تطوير جسيمات أناستروزول النانوية لإدارة توصيل عقار أناستروزول عبر الجلد كبديل للطريق الفموي ولزيادة امتثال المريض.

الطريقة: تم تصنيع الجسيمات النانوية أناستروزول عن طريق الترسيب النانوي باستخدام Kollicoat MAE100-55 كبوليمر والبولوكسامير 188 ، والبولي فينيل بيروليدون- K30 ، وهيدروكسي بروبيل ميثيل السليلوز E5 كمثبتات. تم فحص تركيزات البوليمر والمثبت وأنواع المثبت لتأثيرها على العوامل الفيزيائية للجسيمات النانوية مثل حجم الجسيمات ، جهد الزيتا ، كفاءة تحميل الدواء والانطلاق في المختبر. كما تم إجراء الفحوصات الشكلية والتوافق ، بالإضافة إلى فحص النفاذية خارج الجسم الحي عن طريق جلد بطن الفئران للتحقق من تأثير الإبر الدقيقة البوليمرية الصلبة على تدفق الدواء.

النتائج: أظهرت النتائج أن الترسيب النانوي يمكن أن يصنع جزيئات نانوية بوليمرية. تراوحت الجسيمات النانوية البوليمرية المحضرة في الحجم من 47.41 ± 10.1 نانومتر إلى 541.3 ± 23.6 نانومتر وكان لها إمكانات زيتا سالبة. تراوحت كفاءة تحميل الدواء من 37.67٪ إلى 76.3٪. شوهد شكل كروي وموحد في المجهر الإلكتروني النافذ للصيغة (F2). تم اختيار الصيغة (F2) لمزيد من التقييم نظرًا لصغر حجم الجسيمات ، ونسبة كفاءة تحميل الدواء العالية ، ونمط الإطلاق لمدة 4 ساعات. لم يأخذ تحليل التوافق في الاعتبار تفاعل أناستروزول مع المكونات الاخرى. وجدت دراسة التخلل أن إبر البوليمر المجهرية تزيد من تغلغل الدواء في جلد الفئران مقارنة بالجسيمات النانوية.

الخلاصة: الجمع بين الجسيمات النانوية البوليمرية والإبر الدقيقة زاد من الامتصاص عبر الجلد واختراق أناستروزول ، كبديل للطريق الفموي ، لزيادة امتثال المريض وتقليل الآثار الجانبية.

## Introduction

Drug delivery through the skin has become an increasingly common practice in recent years. Any medication that is applied topically and is intended to enter the bloodstream through the skin is included in the category of transdermal drug delivery systems. By absorption through the skin and into the bloodstream, transdermal drug administration allows for systemic and tissue effects. Not only it is convenient for the patient, but it also avoids first-pass metabolism, minimizes variation in medication blood concentration through regulated distribution over time, and can be used when oral dosing is unappropriate. These features are remarkable, but the skin's impermeable nature creates a physiological barrier that must be overcome [1].

Enhancing skin permeability, modulating medication release, and protecting delicate molecules from degradation are just few reasons why polymeric nanoparticles are becoming increasingly popular. Unfortunately, their contribution to the transdermal sector is limited by their inability to penetrate intact stratum corneum, since it is confined to hair follicles, providing depots for cutaneous drug delivery in a sustained manner [2]. Creating pores using polymer microneedles is a common pre-treatment technique. For example, needles penetrate the skin and create temporal micron-sized channels through which the medicine can be absorbed by applying patches, cream, ointments and gels. This improves the penetration of drugs. To demonstrate a systemic and tissue effect, the substance is absorbed by the vasculature. It can also be used to affect a specific area [3].

Recent interest has grown in microneedles, a micron-scale permeation enhancer comprised of arrays of microscopic projections on a baseplate. Polymer microneedles are used to produce pores on the skin before treatment [4]. Needles penetrate the skin to create temporary micron-sized channels via which high molecular weight drugs, hormones, and nanoparticles can be absorbed by patches, lotions, ointments, and gels. It stimulates drug use. This can also target a specific location under skin layer [5].

Anastrozole (ANA) is a nonsteroidal aromatase inhibitor authorized to treat breast cancer and metastatic disease. Estrogen makes breast cancer worse

[6]. Several studies demonstrate that postmenopausal women's tissue estrogen levels are 10 to 20-fold higher than plasma levels. Limiting estrogen in breast tissue is more effective than in the blood. ANA exhibits only 80 % of oral bioavailability due to first pass metabolism, very slightly soluble in water (0.53 mg/ml at 25 °C) [7]. Therefore, anastrozole possesses all the ideal properties needed for transdermal distribution, including solubility of 0.5 mg/ml, partition coefficient of 3.5, molecular weight of 293.3 Daltons, and dose of 1mg [8].

We attempted to achieve the study's goal by producing anastrozole as polymeric nanoparticles (NPs) with improved stability and delivering them transdermally via microneedles as an alternative to the oral route and to increase patient compliance.

## Materials and Methods

### Materials

Anastrozole was purchased from Hyper Chem, China. kollicoat MAE 100-55 provides as gift from Basf SE, 67056 ludwigshafen Germany. Polyvinyl Pyrrolidone K30 (PVP K30) from Hi-Media Lab. Ltd. India. Ethanol was supplied from Sigma-Aldrich, Germany. Cold Polyvinyl Alcohol(PVA), was purchased from India Central drug house. HPMC E5 was supplied from Provizer Pharma, India. Sodium acetate, acetic acid, and phosphate buffered (pH 7.4) have been got from Merck, Germany, Dialysis membrane 8-14 kDa was supplied from Hi-Media-Lab Pvt. Ltd India.

### Anastrozole Polymeric Nanoparticle Preparation

The nanoprecipitation process was used to create anastrozole polymeric nanoparticles. In 3 mL of ethanol, a water-miscible solvent, ANA and polymer were dissolved; the resulting ANA-polymer dispersion, which represents the organic phase, was then injected by 23 G 1 ¼ (0.6 × 31.8 mm) at 37°C at a rate of 0.5 mL/min into the external aqueous phase (30 mL of acetate buffer pH 4.5) containing various stabilizer. Due to the formation of nanoparticles, The dispersion's color changed to a milky opalescence; evaporation at 40 °C for 30 minutes with a magnetic stirrer removed any

residual organic solvent [9]. After being centrifuged at 4500 rpm for 10 minutes and washed with deionized water, the resulting dispersion was lyophilized and stored for future use . The components of the developed ANA nanoparticle formulations are mentioned in the table (1).

**Table 1: Anastrozole Nanoparticles Formulas Components**

| Formula code | Drug amount (mg) | Kollicoat MAE100-55 amount (mg) | Drug: polymer ratio | Stabilizer w/v% | | |
|---|---|---|---|---|---|---|
| | | | | Poloxamer188 | HPMC E5 | PVP K-30 |
| F1 | 10 | 20 | 1: 2 | 0.5 | - | - |
| F2 | 10 | 20 | 1: 2 | 1 | - | - |
| F3 | 10 | 20 | 1: 2 | 2 | - | - |
| F4 | 10 | 5 | 1: 0.5 | 1 | | |
| F5 | 10 | 40 | 1: 4 | 1 | | |
| F6 | 10 | 20 | 1: 2 | | 1 | |
| F7 | 10 | 20 | 1: 2 | | | 1 |

## Anastrozole Polymeric Nanoparticle Characterization

### Particle size, polydispersity index and zeta potential are measured

Using dynamic light scattering (DLS) techniques (Malvern, zetasizer, ultra, USA) at a scattering angle of 90° at room temperature, particle size (PS), zeta potential (ZP), and polydispersity index (PDI) were determined for nanoparticles. Triplicate measurements were performed for each sample [10].

## ANA Polymeric Nanoparticles Drug Content Determination

To measure quantity of ANA was in each formulation, we diluted 1 mL of polymeric nanoparticle dispersion with ethanol until got 10 mL in a 100 mL volumetric flask. After 2 hours of sonication, a 0.22 µm syringe filter was used to remove any remaining nanoparticles. Finally, the sample was diluted

with DW to the required concentration, and it was determined spectrophotometrically by measuring the UV absorbance at 215 nm, which is the employing λmax [11].

**Measurement of entrapment efficiency**

The entrapment efficiency (EE%), which correlates to the percentage of ANA encapsulated within the nanoparticles, was indirectly evaluated by measuring the concentration of free ANA in the dispersion medium. The amount of free drug was calculated using an ultrafiltration technique [12]. To be more precise, 2 ml of ANA-NPs dispersion were placed in the top chamber of an Amicon Ultra-4 centrifugal tube fitted with a molecular cut off (3KDa), and the tube was spun for 40 minutes at 4500 rpm. The ultrafiltration containing the free drug and the concentration of unentrapped ANA was then determined using UV-spectrophotometer at 215 nm analysis. The (EE%) was determined using the equation equation1 :

$$EE\% = \frac{Mt-Mf}{Mt} \times 100 \qquad \text{(Eq. 1)}$$

Where EE % is the % of entrapment efficiency, Mt is total quantity of ANA added, and Mf is the free quantity of the ANA that passes through the ultra-filter of Amicon (unentrapped drug) [13].

***In-Vitro* ANA release study from polymeric nanoparticles**

The dissolution profiles of ANA polymer nanoparticles were investigated. 3 mL of ANA polymeric nanoparticles dispersion, equivalent to 1 mg of ANA; was placed in an 8-14 kDa molecular weight cutoff dialysis membrane sac that had been pre-immersed in phosphate buffer pH 7.4 including 0.1 v/v% tween 80 (as dissolution media for 8 hours), and the open ends of the sac were tied closed to prevent ANA loss. The sac was then placed in a 50-ml plastic sample test tube with a screw cap containing 45mL of dissolution medium, which was stirred with a water bath shaker at 100±2 rpm [14]. The temperature of the media was kept constant at 25 ± 1 °C. Throughout the experiment, 2 mL aliquots were taken out of the medium of release and replaced with new medium to keep the sink at a constant level; the collected 2 mL was filtered by a 0.22µm syringe filter and then

spectrophotometrically analyzed at 210 nm, which is the confirmed maximum of ANA. The total amount of drugs released was computed. The values reported are the average of three replicates [15].

## Characterization of polymeric nanoparticle morphology

### Transmission electron microscopy (TEM) analysis

Transmission electron microscopy is a technique used to examine the internal structure of a nanoparticle (size and morphology). The sample was placed on a carbon-coated copper grid and allowed to stand at room temperature for 90 seconds to form a thin layer. The samples were examined and photomicrographs were taken using various appropriate magnifications after the grid had properly dried in the air [16].

### Differential Scanning Calorimetry (DSC)

DSC was used to investigate the thermal behavior of the drug, a physical mixture of ANA and polymer in a 1:1 ratio, and the specified formula. The DSC experiment was carried out using thermal analysis instruments (STD Q 600 V20.9 Build 20, USA). The tests were carried out by inserting (4 mg) of into standard aluminum pans in an unusual manner. The temperature was then gradually increased at a rate of 10 °C/min from 25 °C to 350 °C. An empty pan sealed in the same manner as the sample was used as a control [17].

### Application of Microneedles and EX-*Vivo* Permeation Research

Polymeric microneedles made of PVA were used to pierce freshly extracted abdominal rat skin, followed by an ex vivo permeation study through microneedle treated abdominal rat skin. In an ex vivo setting, the Franz diffusion cell was used to investigate ANA polymeric nanoparticle dispersion in rat abdomens removed from the body [18]. To maintain sink conditions, the receptor chambers were filled with 66.5 mL of phosphate buffer pH 7.4 (containing 0.1% v/v tween 80). In which the temperature was kept constant at 37±1 °C, and the medium in the receptor was agitated at 100 rpm with a magnetic stirrer. The donor chamber was partitioned off by gluing the stratum corneum side of the rat skin to the donor chamber. A

dispersion of polymeric nanoparticles equivalent to 1 mg of anastrozole was added to the donor compartment. In order to keep the permeation medium from drying out, the sample arm and donor chamber were covered with Parafilm M®; aliquots of 2 mL of sample were removed from the receptor compartment at 0.5, 1, 1.5, 2, 2.5, 3, 4, 5, 6, 7, and 8 hours and replaced with the same volume of receptor fluid as quickly as possible [19]. The withdrawn sample was filtered, and the amount of ANA that permeated the rat skin at various time intervals was determined using spectrophotometric analysis at 210nm.The experiment was repeated using abdominal rat skin without microneedles as a control, and the permeation test was used by applying 3mL of ANA nanoparticle dispersion in the donor compartment, which is equivalent to 1 mg of anastrozole, while fixing the same testing factors; like flux of steady-state and coefficient of permeation were also determined [20].

**Analysis of data using statistical methods**

The experimental results are presented as a mean of triplicate models ± SD, and One-way analysis of variance was used to analyze the data (ANOVA) to see if the applied component changes are statistically significant at ($P<0.05$) [21].

**Results and Discussion**

**Effect of Formulation Variables on ANA Nanoparticle Physical Properties**

The nanoprecipitation method was used to create ANA polymeric nanoparticles because it is simpler, more energy-efficient, and faster than other methods. This method can benefit ethanol or acetone-soluble substances [22]. Furthermore, it only requires one step of preparation, which is polymer interfacial deposition after rapid diffusion of the miscible solvent to the external antisolvent. Kollicoat® MAE 100-55 was used to make polymeric ANA-nanoparticles. Kollicoat MAE polymers dissolve at pH values greater than 5.5 and have a slightly acidic nature, elucidating pH-dependent medication release properties and form nanodispersions with a negative charge [23].

Table 2 summarizes the results of an extensive investigation into the effects of varying preparation factors on the particle size, polydispersity index, zeta potential, and entrapment effectiveness of nanoparticles. The particle size ranged between 47.41±10.1and 541.3±23.6. Simultaneously, the polydispersity index value lies between 0.0045±0.001and 0.322±0.022 which indicated as mono-dispersion properties.

**Table 2: Physical Properties of the Prepared ANA-Nanoparticles**

| Formula code | Particle size *(nm) | PDI* | Zeta potential* (mV) | EE%* |
|---|---|---|---|---|
| F1 | 78±13.1 | 0.2327±0.012 | -3.935±0.023 | 73±1.5 |
| F2 | 52.49±7.9 | 0.1915±0.065 | -2.71±0.0012 | 74.5±5.6 |
| F3 | 47.41±10.1 | 0.2759±0.074 | -1.962±0.00033 | 63.2±1.9 |
| F4 | 95.2±11.2 | 0.322±0.022 | -4.492±0.098 | 62.3±4.2 |
| F5 | 72.32±9.13 | 0.21±0.051 | -3.936±0.0083 | 76.3±2.1 |
| F6 | 541.3±23.6 | 0.0807±0.004 | -7.318±0.0041 | 73±1.9 |
| F7 | 170.1±18.18 | 0.0045±0.001 | -11.8±0.0056 | 37.67±5.3 |

Mean± Standard deviation (n=3)

Figure 1 explains how particle size is affected by polymer concentration, stabilizer concentration, and stabilizer type.

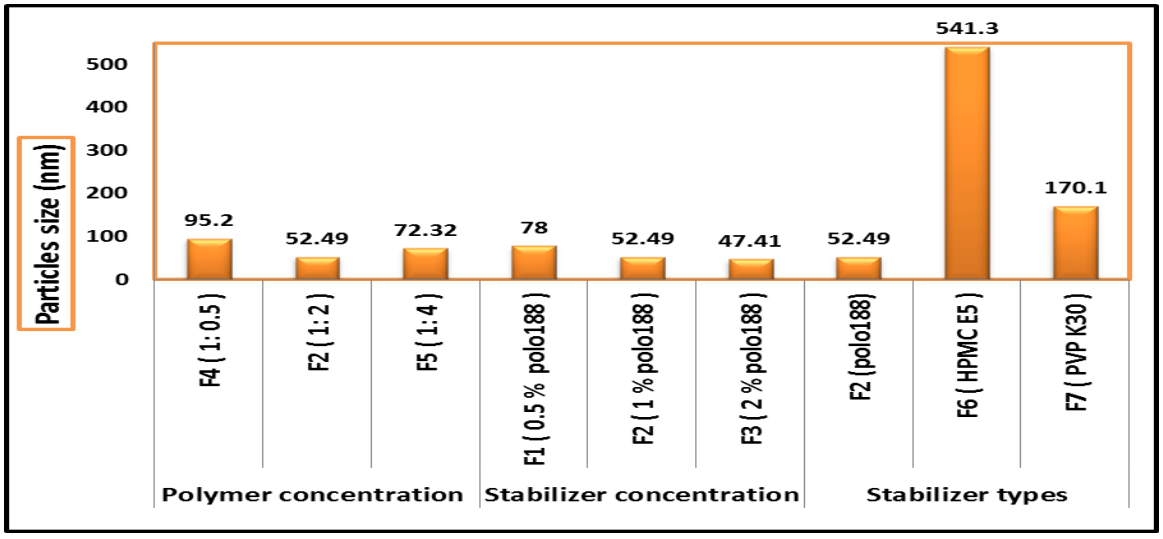


**Figure 1: Particle size and polydispersity index of the prepared formulas**

Effect of polymer concentration on particle size of ANA polymeric nanoparticle. By altering the drug: polymer ratio (1:0.5 in (F4), 1:2 in (F2), and 1:4 in (F5)), the resultant particle size was investigated. The results showed that increasing polymer content affected particle size significantly ($p<0.05$). F4 has the biggest particles (95 nm) due to a low drug: polymer ratio (1:0.5), given the polymer's role in creating nanoparticles, the concentration of polymer utilized was inadequate to start particle formation and nucleation; hence, the drug and polymer form a wide, uneven agglomeration. Particle size and polydispersity index reduced when drug: polymer ratio in formulations (F2) grew to 1:2, suggesting that the polymer concentration was sufficient to surround the drug molecule and create homogeneous particles [24]. Increasing the concentration of dissolved polymer in (F5) with a drug: polymer ratio of (1:4) increased organic phase viscosity, decreased stirring efficiency, and restricted polymer diffusion into the external phase, as a result of which particle size increases [25].

Figure 1 depicts an examination of the influence of stabilizer concentration on particle size, raising the concentration of poloxamer 188 (polo188) decreased particle size significantly ($P<0.05$). Polo188 was utilized as a stabilizer at 0.5%, 1%, and 2% w/v of the aqueous phase in formulations (F1, F2, and F3), respectively. It is often employed as a stabilizer because of its capacity to adsorb on nanoparticle surfaces and protects the generated particles with a thick coating, avoiding coalescence by lowering their interfacial energy [26]. Viscosity of the external phase increases with stabilizer concentration, making particle collisions more difficult. Since 0.5% polo188 in (F1) wasn't enough to cover the particles' surfaces, they clumped together and made big particles [27]. The particle size was reduced by raising the concentration of polo188 to 1% in (F2) and the stabilizer to 2% in (F3), demonstrating that the stabilizer molecules contained the drug particle surface. Explained by the fact that when stabilizer concentration increases, external phase viscosity also increase. The polydispersity index value falls significantly with decreasing stabilizer concentration at constant drug concentration ($p<0.05$). Particle size distribution can be quantified using the polydispersity index [28].

Different stabilizer types (Polo188, HPMC E5, and PVP K30) were tested on ANA nanoparticles using (F2, F6, and F7), respectively. Chosen a stabilizer impacted formulation particle size significantly ($p<0.05$). All stabilizers produced nanoparticles between 52.49 and 541.3 nm. Stabilizers inhibit nanoparticle clumping by creating a mechanical and thermodynamic barrier [29]. Type and ratio of stabilizers are crucial for a stable preparation. They must form a steric or ionic barrier and wet drug particle surfaces [30]. The hydrophobic PPO group of polo188 prevents crystal formation, while the hydrophilic PEO chains produce a steric barrier upon aggregation. The drug molecule and poloxamer188 (F2) bond hydrophobically [31]. HPMC in (F6) gives steric stability. Due to the solution's viscosity, drug particles are absorbed by a thick, wide layer that swells, increasing particle size [32]. PVP-k30 (F7) did not produce nanoparticles with small particle sizes, possibly because it has only one hydrogen-bonding carbonyl group per molecule unit [33].

In colloidal systems, the zeta potential measures interparticle repulsion to gauge system stability. All formulations with anionic pH-sensitive polymers have an external aqueous pH of 4.5. Ionization of its carboxyl group led to a low negative zeta potential [34].

For system stabilization and to prevent particle agglomeration during storage, higher zeta potentials are preferred, however the prepared system's stability at lower zeta potentials can be explained by the applied stabilizer's steric stabilization rather than electrostatic stabilization. When a stabilizer is added to a system, the plane of shear moves away from the particle surface, lowering the zeta potential [35].

Table (2) indicates a wide range of entrapment efficiencies (37.67% to 76.3%). The drug: polymer ratio enhanced EE% of ANA significantly ($p<0.05$). The formulation (F5) with the highest EE (76.3%) has a 1:4 drug: polymer ratio. Increasing organic phase viscosity reduces drug diffusion from the organic to aqueous phase, entrapping more pharmaceuticals in NPs [36]. The polo188 stabilizer concentration was increased from 0.5% to 2% w/v lowered EE at constant drug: polymer ratios (1:2 and 1: 4) Small particles exhibited low entrapment efficacy, and their size affected the drug's

%EE. As polo188 increases, polo attachment to nanoparticle polymer shells may increase, enhancing hydrophilic characteristics. Hydrophilic nanoparticles may cause medication loss in solution, and this lead to lowering % EE [37].

How the ratio of drug to polymer effects on ANA release behavior from nanoparticles was examined using (F2) and (F5) with a drug: polymer ratio of (1:2) and (1:4), respectively. The amount of ANA released from nanoparticles dropped ($p>0.05$) in a non-significant manner as the polymer ratio grew. Formula F5, generated with the highest drug:polymer ratio of (1:4) released around 85% of its payload after 4 hours, in contrast to Formula F2's total release at that time [38]. As shown in figure (2). These results could be attributed to pH, temperature, and polymer nature; all important drug release factors. Kollicoat MAE copolymers are soluble in solutions with a pH greater than 5.5. Phosphate buffer pH 7.4 as (dissolution media including 0.1% tween 80) causes the coated layer to swell and dissolve proportionally to pH above 5.5 [39].

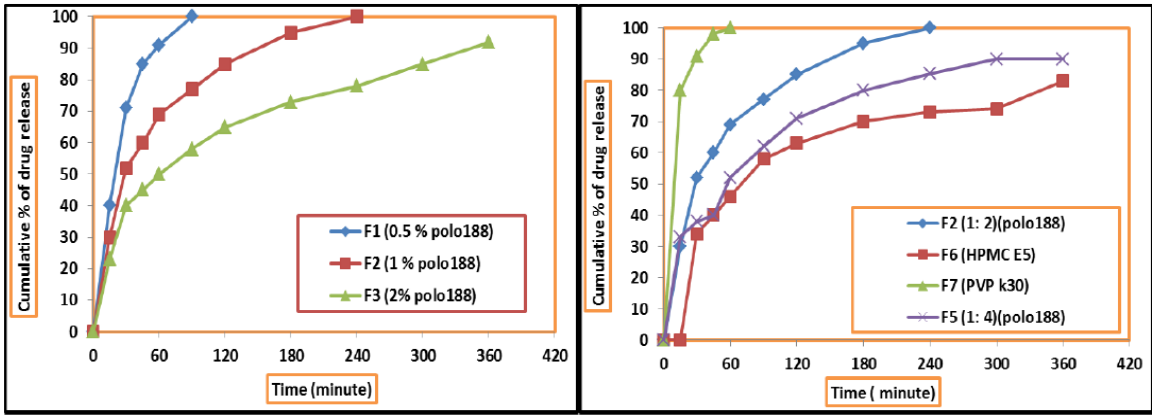


**Figure 2: The Influence of preparation parameters on cumulative % of drug release**

Since in-*vitro* drug release studies showed that the amount of drug released decreased significantly ($p<0.05$) as the stabilizer ratio was increased at a constant drug:polymer ratio of (1:2) [40]. This was studied using three different preparations (F1, F2, and F3) with stabilizer concentrations of (0.5%, 1%, and 2%w/v polo188), respectively. Instead of homogenous nanoparticles, AN-4 is composed of clusters of polymer and stabilizer, and

their release is quick. When pH increases it causes polymer swelling and erosion [41]. The polymer rapidly disintegrated due to poor particle stability, resulting in full drug release after 1.5 hours. The proper stability of nanoparticles allowed F2 to releases medication for 4 hours and F3 to releases just 78% after 4 hours. Polo188 reduces drug-to-dissolution medium contact area, which may explain this action. Poloxamer's gelling effect at high concentrations may be to blame [40].

As shown in Figure 2, the release profiles of F2, F6, and F7 stabilized with Polo188, HPMC E5, and PVP K30, respectively, were used to study the effect of stabilizer type on drug release from ANA nanoparticles. The results show difference in drug release ($P<0.05$) between stabilizer types. The faster release of F7 stabilized by PVP K30 may be related to the pore-former in the coating-layer, which enhances the polymeric matrix's exposure to the release medium and its erosion and drug solubility [42]. Despite the pH-sensitive polymer, F6 stabilized with HPMC E5 showed longer release than F2 stabilized by polo188. The larger particle size of F6 explains this. By expanding into a gel when wet, HPMC slows drug release from the matrix [43]. Due to its tiny particle size, good entrapment efficiency, and capacity to completely release drug loading in a continuous pattern within 4 hours, F2 was chosen as the optimum formula and subjected to additional testing.

## Characterization of Polymeric Nanoparticles' Morphology

The morphology of the chosen nanoparticles (formula F2) was observed at various scales. The images shown in figure 30 (A&B) show that the nanoparticles have a regular spherical shape that is well stabilized by the added stabilizer adsorbed at their surfaces; the particles under study are nano size. As shown in figure 3.

## Differential Scanning Calorimetry (DSC)

The DSC thermogram shows that ANA has a prominent endothermic peak (86.52°C) near anastrozole melting point of 81-83 °C, figure (4-A). This peak shows that the anastrozole utilized is pure. No new peaks were observed in the thermograms of ANA and the polymer-physical mixture used to make nanoparticles and dissolving microneedles (koll.100-55 and

polo188), showing strong drug-polymer compatibility. Figure (4-C) shows that the ANA peaks disappeared, indicating that the medication was entrapped in the polymeric matrix. A new endothermic peak developed at 53.56°C, the plasticizer poloxamer188's melting point [44].

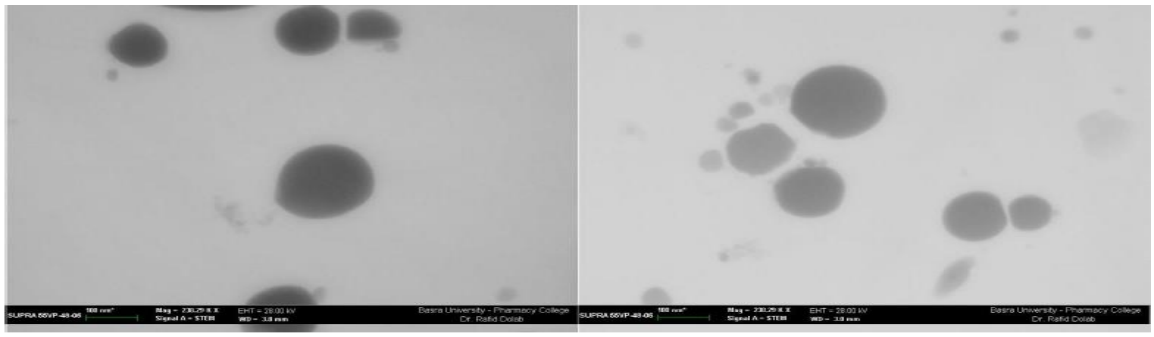

**Figure 3: TEM images of optimize F2 formula**

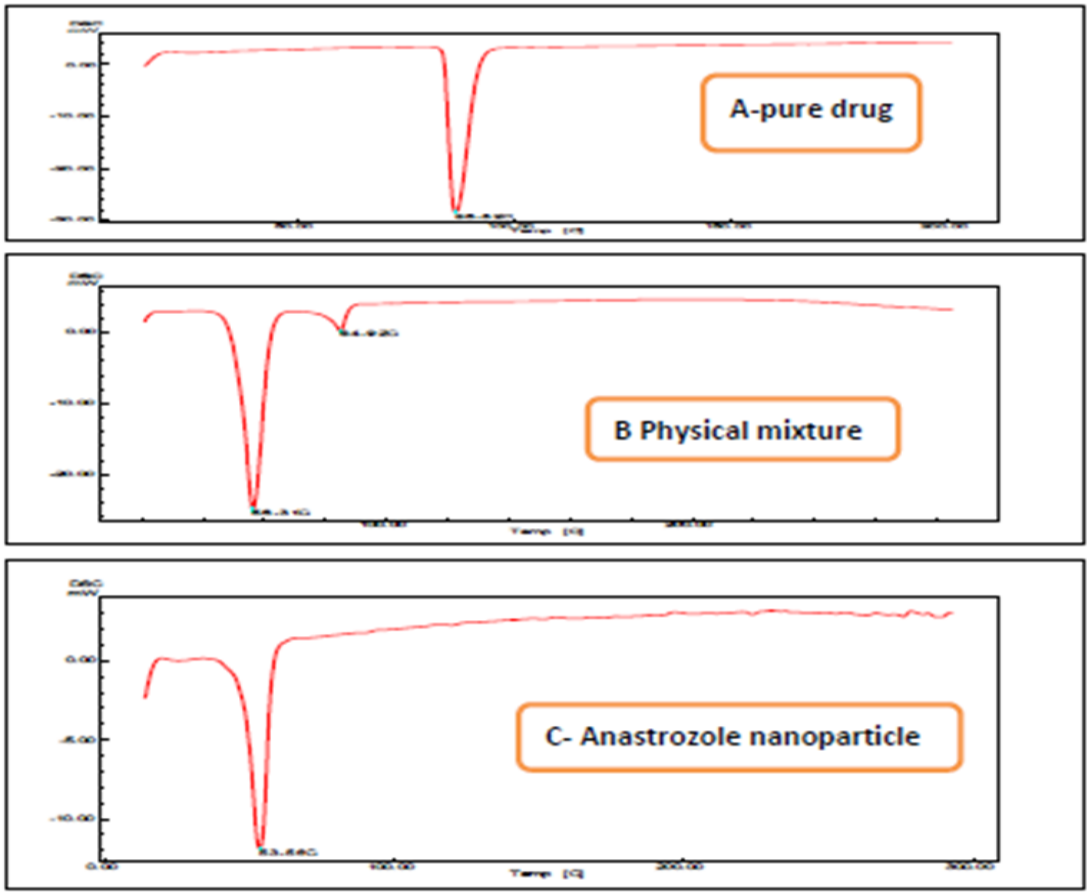


**Figure 4: DSC of A-pure ANA, B- physical mixture and C- anastrozole nanoparticles**

## Powder X-ray diffraction (PXRD)

Figure (5-A) shows strong, high-intensity peaks at diffraction angles 2 of 9.71°, 16.85°, 18.69°, 19.67°, 22.37°, 25.83°, 26.92°, 27.8°, and 29.2°, indicating that ANA is crystalline. The PXRD diffraction pattern of drug-polymer physical combination figures shows ANA peaks with reduced intensity (5-B). The physical combination contained crystalline ANA, indicating no drug polymer interaction. ANA nanoparticles loaded with ANA did not exhibit any of its characteristic peaks at its specific diffraction angle, indicating amorphous form (5-C) [45].

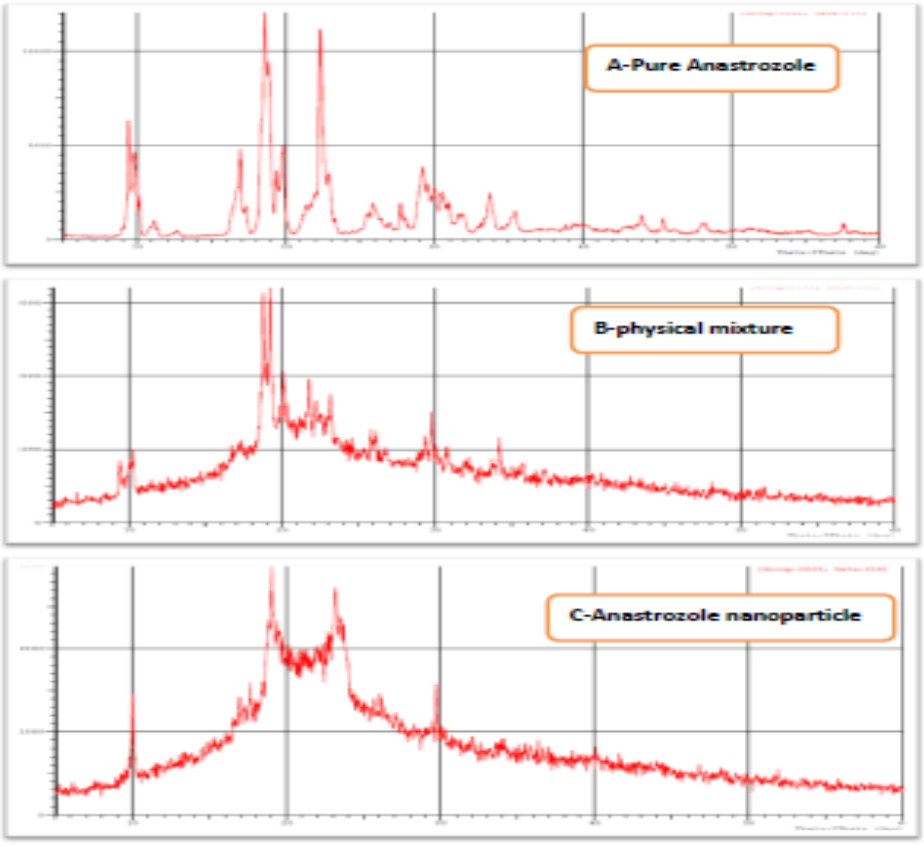


**Figure 5: PXRD of A- pure drug, C- physical mixture and anastrozole nanoparticle**

## Application of Microneedles and Ex-*Vivo* Permeation Analysis

This study compared the penetration of anastrozole nanoparticles via untreated skin to skin treated with polymeric microneedles and evaluated the efficacy of the microneedles in increasing nanoparticle penetration.

After 7 hrs, more than 89.7% of the loaded drug with nanoparticles permeated through the skin previously treated with microneedles. However, at the end of the 8 hours, the amount permeated through naked skin did not exceed 17.2%, indicating a significant difference ($p<0.05$) in the total amount of drug permeated. In both cases, the steady-state flux was calculated using the permeation profile depicted in Figure 6. Polymeric nanoparticles permeated through skin treated with microneedles had a permeation rate of 30.371± 2.64 µg/cm$^2$.hr and bare skin had a permeation rate of 5.6866± 0.12 µg/cm$^2$.hr, respectively. Furthermore, the permeation coefficients were found to be 0.0912± 0.00054 cm/hr and 0.01708± 0.00014 cm/hr, and a significant increase ($p<0.05$) in the steady-state flux of nanoparticles through the skin treated with microneedles was observed [46]. Microneedles can form micro-channels larger than nanoparticles' diameter, which increases penetration by 5.2 times. The trans-appendageal pathway is the sole known mechanism for nanoparticle administration through bare skin [47].

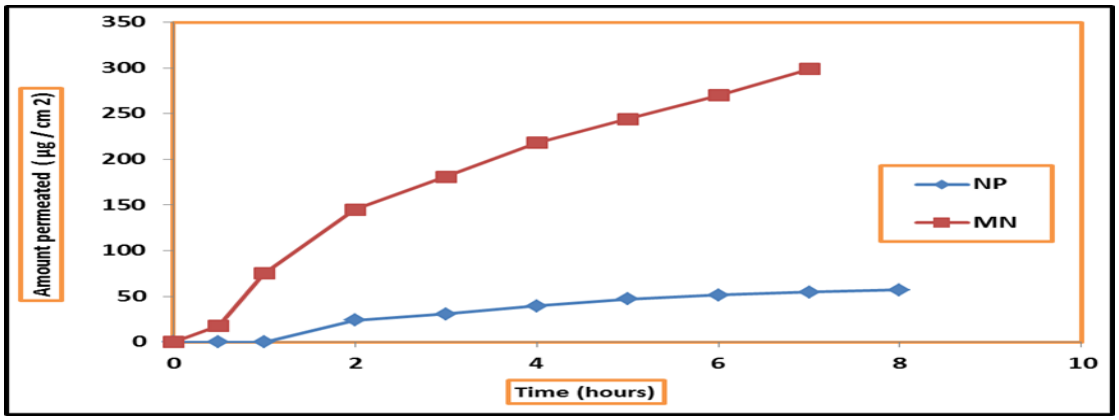


**Figure 6: Permeation profile of ANA nanoparticles through skin treated with microneedles and bare skin**

## Conclusion

Anastrozole permeation amounts from polymeric nanoparticle dispersion (F2) through skin previously treated with polymeric microneedle and through bare skin (untreated with microneedle) were 89.7% and 17.2%, respectively. These findings suggest that using a combined strategy of producing anastrozole as polymeric nanoparticles with improved stability

and delivering them transdermally via microneedles can form micro-channels larger than the nanoparticles' diameter, increasing penetration by 5.2 folds. Anastrozole has all of the ideal properties for transdermal distribution, including a solubility of 0.5 mg/ml, a partition coefficient of 3.5, a molecular weight of 293.3 daltons, and a dose of 1 mg. Anastrozole polymeric nanoparticles for transdermal delivery via microneedles as an alternative to oral administration to increase tissue effect and patient compliance.

## Acknowledgment

We're grateful to the University of Baghdad's Pharmacy Department for supporting this study.

**Conflict of interest**: None

## References

1-Akhtar N, Singh V, Yusuf M, Khan RA. Non-invasive drug delivery technology: Development and current status of transdermal drug delivery devices, techniques and biomedical applications. Biomed Eng Tech. 2020;65(3):243–72.

2-Lam SJ, Wong EHH, Boyer C, Qiao GG. Antimicrobial polymeric nanoparticles. Prog Polym Sci. 2018 Jan;76:40–64.

3-Ali R, Mehta P, Arshad M, Kucuk I, Chang M-W, Ahmad Z. Transdermal Microneedles—A Materials Perspective. AAPS PharmSciTech. 2020 Jan 5;21(1):12.

4-Waghule T, Singhvi G, Dubey SK, Pandey MM, Gupta G, Singh M, et al. Microneedles: A smart approach and increasing potential for transdermal drug delivery system. Biomed Pharmacother. 2019 Jan;109:1249–58.

5-Vicente-Perez EM, Larrañeta E, McCrudden MTC, Kissenpfennig A, Hegarty S, McCarthy HO, et al. Repeat application of microneedles does not alter skin appearance or barrier function and causes no measurable disturbance of serum biomarkers of infection, inflammation or immunity in mice in vivo. Eur J Pharm Biopharm. 2017 Aug;117:400–7.

6-Chi D, Singhal H, Li L, Xiao T, Liu W, Pun M, et al. Estrogen receptor signaling is reprogrammed during breast tumorigenesis. Proc Natl Acad Sci. 2019;116(23):11437–43.

7-Zhang Z, Tsai P, Ramezanli T, Michniak-Kohn BB. Polymeric nanoparticles-based topical delivery systems for the treatment of dermatological diseases. Wiley Interdiscip Rev Nanomedicine Nanobiotechnology. 2013;5(3):205–18.

8-Vidya K, Lakshmi PK. Cytotoxic effect of transdermal invasomal anastrozole gel on MCF-7 breast cancer cell line. J Appl Pharm Sci. 2019;9(3):50–8.

9-Kumar A, Sawant KK. Application of multiple regression analysis in optimization of anastrozole-loaded PLGA nanoparticles. J Microencapsul. 2014;31(2):105–14.

10-Sundar VD, Dhanaraju MD, Sathyamoorthy N. Preparation and characterization of anastrozole loaded magnetic poly (epsilon-caprolactone) microspheres for anticancer activity. Der Pharm Lett. 2016;8(10):118–28.

11-Joshi HD, Ghode GS, Gore SB. Efficiency of letrozole loaded PLGA nanoparticles on sex reversal of Poecilia reticulata (Peters, 1859). J Appl Nat Sci. 2015;7(1):394–9.

12-Lv Y, He H, Qi J, Lu Y, Zhao W, Dong X, et al. Visual validation of the measurement of entrapment efficiency of drug nanocarriers. Int J Pharm. 2018;547(1–2):395–403.

13-Vu MT, Nguyen DTD, Nguyen NH, Le VT, Nguyen TH, Cong TD, et al. Development, characterization and in vitro evaluation of paclitaxel and anastrozole Co-loaded liposome. Processes. 2020;8(9):1110.

14-Ghadge D, Nangare S, Jadhav N. Formulation, optimization, and in vitro evaluation of anastrozole-loaded nanostructured lipid carriers for improved anticancer activity. J Drug Deliv Sci Technol. 2022 Jun;72:103354.

15-Singh A, Vaishagya K, K Verma R, Shukla R. Temperature/pH-triggered PNIPAM-based smart nanogel system loaded with anastrozole delivery for

application in cancer chemotherapy. AAPS PharmSciTech. 2019;20(5):1–14.

16-Vekariya KK, Kaur J, Tikoo K. Alleviating anastrozole induced bone toxicity by selenium nanoparticles in SD rats. Toxicol Appl Pharmacol. 2013;268(2):212–20.

17-Miroshnichenko II, Yurchenko NI, Platova AI. Quantitative Determination of Anastrozole by Liquid Chromatography–Tandem Mass Spectrometry. Pharm Chem J. 2013;47(4):231–4.

18-Donnelly RF, Singh TRR, Woolfson AD. Microneedle-based drug delivery systems: microfabrication, drug delivery, and safety. Drug Deliv. 2010;17(4):187–207.

19-Folzer E, Gonzalez D, Singh R, Derendorf H. Comparison of skin permeability for three diclofenac topical formulations: an in vitro study. Die Pharm Int J Pharm Sci. 2014;69(1):27–31.

20-Gwak HS, Oh IS, Chun IK. Transdermal delivery of ondansetron hydrochloride: effects of vehicles and penetration enhancers. Drug Dev Ind Pharm. 2004;30(2):187–94.

21-Assaad HI, Zhou L, Carroll RJ, Wu G. Rapid publication-ready MS-Word tables for one-way ANOVA. Springerplus. 2014;3(1):1–8.

22-Adhikari C. Polymer nanoparticles-preparations, applications and future insights: A concise review. Polym Technol Mater. 2021;60(18):1996–2024.

23-Endale A, Gebre-Mariam T, Schmidt PC. Granulation by roller compaction and enteric coated tablet formulation of the extract of the seeds of glinus lotoides loaded on Aeroperl® 300 Pharma. Aaps Pharmscitech. 2008;9(1):31–8.

24-Bock N, Woodruff MA, Hutmacher DW, Dargaville TR. Electrospraying, a reproducible method for production of polymeric microspheres for biomedical applications. Polymers (Basel). 2011;3(1):131–49.

25-Amado JRR, Prada AL, Duarte JL, Keita H, da Silva HR, Ferreira AM, et al. Development, stability and in vitro delivery profile of new loratadine-loaded nanoparticles. Saudi Pharm J. 2017;25(8):1158–68.

26-Cortés H, Hernández-Parra H, Bernal-Chávez SA, Prado-Audelo ML Del, Caballero-Florán IH, Borbolla-Jiménez F V, et al. Non-ionic surfactants for stabilization of polymeric nanoparticles for biomedical uses. Materials (Basel). 2021;14(12):3197.

27-Bhakay A, Rahman M, Dave RN, Bilgili E. Bioavailability enhancement of poorly water-soluble drugs via nanocomposites: Formulation–Processing aspects and challenges. Pharmaceutics. 2018;10(3):86.

28-Chourasiya V, Bohrey S, Pandey A. Polymeric nanoparticles containing ramipril using biodegradable polymer: preparation, optimisation by 23 factorial design, characterisation and in vitro drug release kinetics. Oxid Commun. 2017;40(4):1355–66.

29-Fan X, Chung JY, Lim YX, Li Z, Loh XJ. Review of adaptive programmable materials and their bioapplications. ACS Appl Mater Interfaces. 2016;8(49):33351–70.

30-Gigliobianco MR, Casadidio C, Censi R, Di Martino P. Nanocrystals of poorly soluble drugs: drug bioavailability and physicochemical stability. Pharmaceutics. 2018;10(3):134.

31-Gandhi A, Jana S, Sen KK. In-vitro release of acyclovir loaded Eudragit RLPO® nanoparticles for sustained drug delivery. Int J Biol Macromol. 2014;67:478–82.

32-Afifi SA, Hassan MA, Abdelhameed AS, Elkhodairy KA. Nanosuspension: an emerging trend for bioavailability enhancement of etodolac. Int J Polym Sci. 2015;2015.

33-Du BD, Phu D Van, Duy NN, Lan NTK, Lang VTK, Thanh NVK, et al. Preparation of colloidal silver nanoparticles in poly (N-vinylpyrrolidone) by γ-irradiation. J Exp Nanosci. 2008;3(3):207–13.

34-Mukhopadhyay P, Mishra R, Rana D, Kundu PP. Strategies for effective oral insulin delivery with modified chitosan nanoparticles: a review. Prog Polym Sci. 2012;37(11):1457–75.

35-Mollakhalili Meybodi N, Mohammadifar MA, Farhoodi M, Skytte JL, Abdolmaleki K. Physical stability of oil-in-water emulsions in the presence of gamma irradiated gum tragacanth. J Dispers Sci Technol. 2017;38(6):909–16.

36-Song X, Zhao Y, Wu W, Bi Y, Cai Z, Chen Q, et al. PLGA nanoparticles simultaneously loaded with vincristine sulfate and verapamil hydrochloride: systematic study of particle size and drug entrapment efficiency. Int J Pharm. 2008;350(1–2):320–9.

37-Sanjula B, Shah FM, Javed A, Alka A. Effect of poloxamer 188 on lymphatic uptake of carvedilol-loaded solid lipid nanoparticles for bioavailability enhancement. J Drug Target. 2009;17(3):249–56.

38-Prada AL, Keita H, de Souza TP, Lima ES, Acho LDR, da Silva M de JA, et al. Cassia grandis Lf nanodispersion is a hypoglycemic product with a potent α-glucosidase and pancreatic lipase inhibitor effect. Saudi Pharm J. 2019;27(2):191–9.

39-Majeed A, Ranjha NM, Hussain M, Rasool MF. Fabrication and evaluation of pH-dependent polymeric microspheres of ivabradine and their in vitro and in vivo studies. Polym Bull. 2019;76(6):3127–51.

40-Arafat M, Sarfraz M, AbuRuz S. Development and In Vitro Evaluation of Controlled Release Viagra® Containing Poloxamer-188 Using GastroplusTM PBPK Modeling Software for In Vivo Predictions and Pharmacokinetic Assessments. Pharmaceuticals. 2021;14(5):479.

41-Tran TT-D, Tran PH-L, Phan ML-N, Van TV. Colon specific delivery of fucoidan by incorporation of acidifier in enteric coating polymer. Int J Pharm Biosci Technol. 2013;9(13):14.

42-Yang M, Xie S, Li Q, Wang Y, Chang X, Shan L, et al. Effects of polyvinylpyrrolidone both as a binder and pore-former on the release of

sparingly water-soluble topiramate from ethylcellulose coated pellets. Int J Pharm. 2014;465(1–2):187–96.

43-Enayatifard R, Saeedi M, Akbari J, Tabatabaee YH. Effect of Hydroxypropyl Methylcellulose and Ethyl Cellulose Content on Release Profile and Kinetics of Diltiazem HCl from Matrices. Trop J Pharm Res. 2009 Nov 24;8(5).

44-Di Nardo G, Cimicata G, Baravalle R, Dell'Angelo V, Ciaramella A, Catucci G, et al. Working at the membrane interface: Ligand-induced changes in dynamic conformation and oligomeric structure in human aromatase. Biotechnol Appl Biochem. 2018;65(1):46–53.

45-Satyanarayana DA, Keshavarao KP. Fast disintegrating films containing anastrozole as a dosage form for dysphagia patients. Arch Pharm Res. 2012;35(12):2171–82.

46-Nair RS, Ling TN, Shukkoor MSA, Manickam B. Matrix type transdermal patches of captopril: ex vivo permeation studies through excised rat skin. J Pharm Res. 2013;6(7):774–9.

47-Wiraja C, Zhu Y, Lio DCS, Yeo DC, Xie M, Fang W, et al. Framework nucleic acids as programmable carrier for transdermal drug delivery. Nat Commun. 2019;10(1):1–12.